

The Arctic Forest of the Middle Eocene

A. Hope Jahren

Department of Earth and Planetary Science, Johns Hopkins University, Baltimore, Maryland 21218; email: jahren@jhu.edu

Annu. Rev. Earth Planet. Sci. 2007. 35:509–40

First published online as a Review in Advance on January 29, 2007

The *Annual Review of Earth and Planetary Sciences* is online at earth.annualreviews.org

This article's doi:
10.1146/annurev.earth.35.031306.140125

Copyright © 2007 by Annual Reviews.
All rights reserved

0084-6597/07/0530-0509\$20.00

Key Words

Metasequoia, Fossil Forest, paleoenvironment, paleosol, relative humidity, biomarker

Abstract

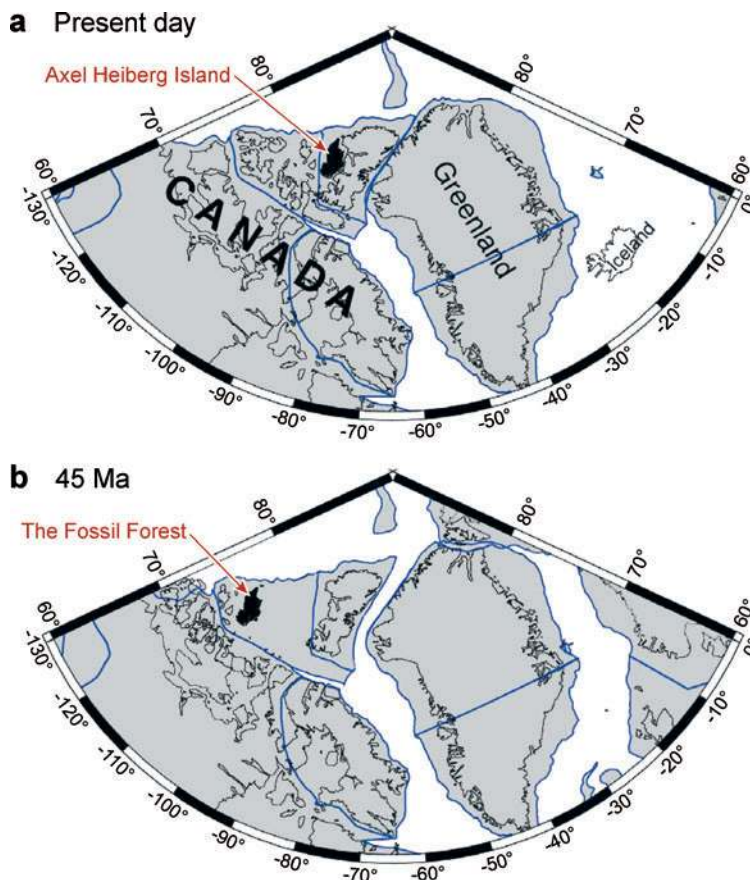
Lush forests, dominated by deciduous conifers, existed well north of the Arctic Circle during the middle Eocene (~45 Ma). The Fossil Forest site, located on Axel Heiberg Island, Canada, has yielded a particularly rich assemblage of plant macro- and microfossils, as well as paleosols—all exquisitely preserved. Methods ranging from classical paleobotany, to stable-isotope geochemistry, have been applied to materials excavated from the Fossil Forest and have revealed layers of diverse conifer forests with a rich angiosperm understory that successfully endured three months of continuous light and three months of continuous darkness. Paleoenvironmental reconstructions suggest a warm, ice-free environment, with high growing-season-relative humidity, and high rates of soil methanogenesis. Methods to evaluate intraseasonal variability highlight the switchover from stored to actively fixed carbon during the short annual growing season.

INTRODUCTION

Between the dramatic warming events of the Paleocene-Eocene transition (~ 55 Ma) (Higgins & Schrag 2006, MacLennan & Jones 2006, Moran 2006, Sluijs et al. 2006) and the large-scale cooling at the Eocene-Oligocene transition (~ 24 Ma) (Dalai et al. 2006, DeConto & Pollard 2003, Grimes et al. 2005, Ivany et al. 2006), there spanned an ~ 21 -million-year-long epoch known as the Eocene. The middle Eocene (~ 49 to ~ 37 Ma) is notable for the extensive landmasses that were located above the Arctic Circle for millions of years. **Figure 1** illustrates the large expanses of continental lithosphere located at high latitudes, during the middle Eocene and compared with the present. In addition, vast expanses of what now constitutes Siberia were located far north of the Arctic Circle. The major tectonic forces of the middle Eocene that are relevant to Arctic regions are illustrated by **Figure 2**, which shows the inception of spreading ridges near what is now Greenland, as well as the continuing opening of the Atlantic Ocean.

Figure 1

Position of tectonic plates at present (*a*) and during the middle Eocene (*b*). Tree wood, leaves, cones, and other fossils excavated from the Axel Heiberg site are the remnants of extensive deciduous conifer forests that were located well above the Arctic Circle ($66^{\circ}33'N$), covering what are now Siberia, Greenland, and northern Canada. Plate boundaries are shown in blue; modern shorelines are indicated by black lines. This image was generated using the Plate Tectonic Reconstruction Service made public by the Ocean Drilling Stratigraphic Network (GEOMAR).



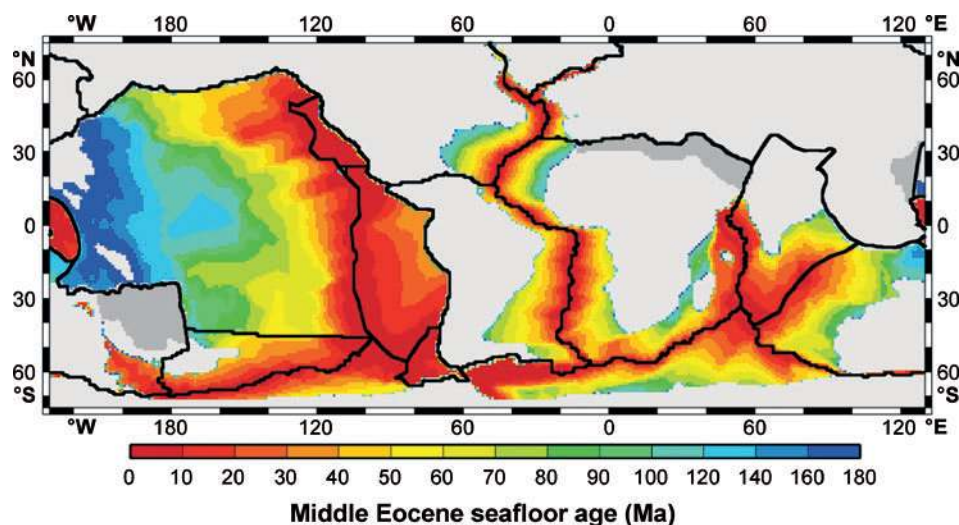


Figure 2

Continental locations and age of the seafloor during the middle Eocene (~45 Ma). The continental lithosphere (*light gray*) is contrasted with the color-coded seafloor; extensive landmasses existed at extreme latitudes. The initiation of spreading ridges defining what would become Greenland, the violent subduction of the remainder of the Farallon plate, and the rapid northward subduction of the Pacific plate beneath Alaska constitute the most important tectonic forces of the time, relative to the Axel Heiberg Island site. Seafloor age was determined from the reconstructions of Xu et al. (2006), which are based on an extrapolation of present-day ages (Müller et al. 1997) backward in time using the history of plate motions defined for the globe by Gordon & Jurdy (1986) and for the western Pacific by Hall (2002). Age could not be determined for regions indicated in dark gray.

THE HISTORY OF THE FOSSIL FOREST

The most important terrestrial fossil locality for the Arctic middle Eocene was found, like most rich fossil sites, purely serendipitously. In 1985, B. Ricketts of the Geological Survey of Canada found mummified Eocene-age plant deposits on Axel Heiberg Island while surveying the area. He informed J.F. Basinger of the site, who made a field excursion that same year to find well-preserved mummified plant remains, including cones, leaves, and wood fragments. The site established by Basinger was a few kilometers from the Fossil Forest locality, which was discovered in 1986 by a helicopter pilot named P. Tudge. Tudge noticed a large concentration of logs and in situ stumps from the air and landed to take a closer look and to take photographs. J. MacMillan of the Geological Survey of Canada told J.F. Basinger of this new site, and in 1986, the first research expedition by paleobotanists to the Fossil Forest was undertaken by J.F. Basinger, J.E. Francis, and J. MacMillan (Basinger et al. 1988).

At present, the Fossil Forest is located on Axel Heiberg Island, which is part of the Arctic Canadian Archipelago in the Nunavut territory of Canada. It is located at 79°55'N, 89°02'W (Geological Society of Canada Map 1301A), far above the Arctic

Figure 3

Satellite image of Axel Heiberg Island, showing the location of the Fossil Forest. Figure courtesy of 2005 Geographic Data Technology Canada, Inc.



Circle ($66^{\circ}33'39''\text{N}$). Axel Heiberg Island is $43,178 \text{ km}^2$ in size and is positioned directly west of Ellesmere Island (**Figure 3**). The Fossil Forest lies on the eastern side of Axel Heiberg Island between the Eureka Sound and the Princess Margaret Mountain Range (**Figure 4**). For reference, the site is located approximately 1500 km



Figure 4

Panoramic photograph of the Fossil Forest field site. The dark sedimentary layers are rich with abundant plant fossils representing all components of the middle Eocene Arctic deciduous conifer forest.

north of the Arctic Circle and is approximately 1000 km north of the most northern part of Alaska.

The modern climate of the Fossil Forest site (also known as Napartulik) is characterized as an arctic climate with long, cold winters and short, cool summers. The mean annual temperature (MAT) is estimated to be -20°C , and the site receives an annual precipitation of 65 mm, 70% of which falls as snow (Tarnocai & Smith 1991). Permafrost underlies the whole region. The Fossil Forest is preserved within the lignitic strata of the Upper Block Coal Member of the Buchanan Lake Formation. This Member consists of repeating fining-upward sequences of sandstones, mudstones, siltstones, and lignites (Ricketts 1991). The strata have likely been exposed by incision in response to isostatic rebound since the major Pleistocene glaciations (Ricketts 1987). The modern rate of surface erosion from these unconsolidated sediments is high, averaging a minimum of 3 mm per year (Bigras et al. 1995).

THE GEOLOGICAL CONTEXT OF THE FOSSIL FOREST

Axel Heiberg Island, where the Fossil Forest is located, has been reconstructed to be located at 78.6°N ($\pm 1.6^{\circ}\text{N}$) during the period of 55 to 40 Ma (Irving & Wynne 1991, McKenna 1980). This position, north of the Arctic Circle, implies a winter of continuous darkness lasting 115 days, a summer of continuous light lasting 130 days, and very short transitional seasons (spring and fall), each lasting only approximately 60 days (Figure 5). Despite the extreme nature of the light environment, the middle Eocene Fossil Forest was teeming with diverse photosynthetic organisms, including abundant trees. The exquisite preservation of these mummified plant remains is stunning and has allowed for a wide range of approaches to paleoenvironmental reconstruction, ranging from the use of classical paleontological techniques to involved stable-isotope geochemistry.

Jahren & Sternberg (2002) documented 33 fossil-bearing layers within ~ 150 vertical stratigraphic meters of sediment. Layers ranged from a few centimeters to several meters in thickness and contained a mixture of wood and leaf macrofossils from both conifer and angiosperm organisms. Greenwood & Basinger (1993) proposed that the accumulation rates of peat at the site were approximately $1\text{--}2\text{ mm year}^{-1}$ based on accumulation rates of modern *Taxodiaceous* swamps. However, the remnants of these peats (now expressed as lignite layers) have been variably compacted over time. Therefore, determining the original peat thickness and calculating time intervals of deposition proves elusive, given the obvious diagenesis. Kojima et al. (1998) estimated minimum accumulation rates of lignites by assuming (a) a constant leaf-area index and (b) that at least half the mass of *Metasequoia* leaves had been preserved. This approach resulted in a minimum accumulation rate of 0.8 mm year^{-1} . Comparing this calculated value to modern rates of peat accumulation using the ^{14}C method is difficult because of uncertainties associated with compaction ratios within lignites. Most workers do agree, however, that the Axel Heiberg middle Eocene forest was highly productive (e.g., Williams et al. 2003b).

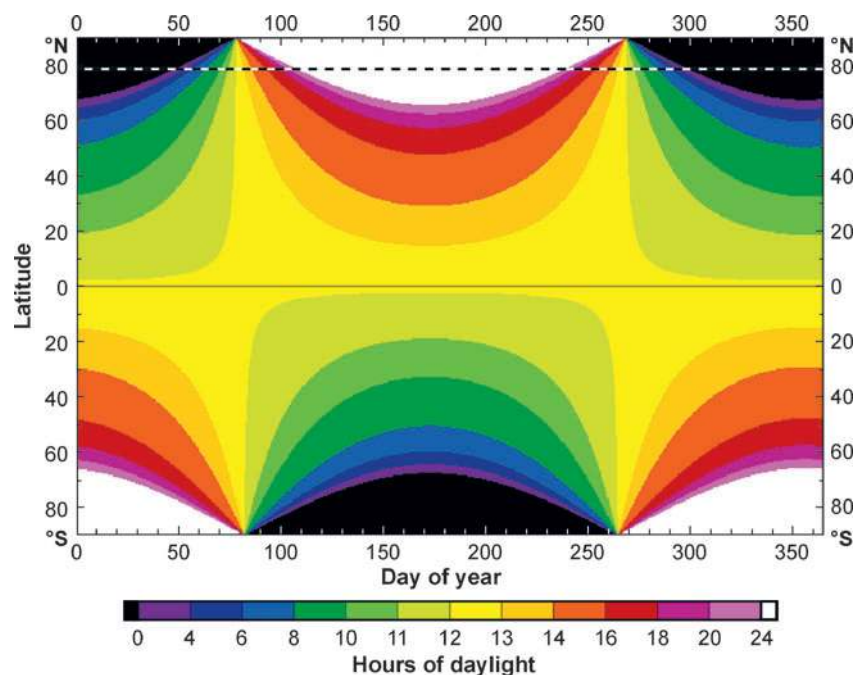


Figure 5

Hours of daylight shown as a function of calendar day of the year, calculated using Forsythe et al.'s (1995) CMB model. White and black represent periods of constant daylight and constant night, respectively. The black-and-white dashed line is located at 78.6°N, the reconstructed location of the Fossil Forest during the middle Eocene (Irving & Wynne 1991, McKenna 1980). The timing of sunrise and sunset are defined by the instant when the top of the sun appears even with the horizon for zero elevation and nonsloping ground, consistent with the U.S. government definition. Because this definition of daylight includes the time during which the sun crosses the horizon, day length at the equator exceeds 12 h. On the basis of these data, we estimate that the Fossil Forest of the Eocene Arctic experienced seasons as following: winter (continuous darkness) = 115 days, spring = 60 days, summer (continuous light) = 130 days, and fall = 60 days.

THE AGE OF THE SITE

The geologic age of the Fossil Forest is generally accepted to be middle Eocene (~45 Ma). This determination arises from several lines of evidence. The earliest observations concerned the Eureka orogeny that formed the Princess Margaret Range, which still forms the central ridge of Axel Heiberg Island (**Figure 3**). Ricketts (1987) described the Buchanan Lake Formation as the strata containing extensive tree fossils and noted that it unconformably overlies rocks as old as Early Triassic in age and as young as middle Eocene in age. From this, Ricketts concluded that the Fossil Forest was derived from sediment shed during the orogeny, which he placed during the middle Eocene.

Although the Fossil Forest is rich with plant fossils of all types, limited age determination may be made on the basis of these assemblages. After an extensive examination of the palynomorphs that could be recovered from Fossil Forest strata, McIntyre (1991) concluded that the pollen flora was most similar to middle Eocene assemblages, but did not discount a late Eocene age. This study was later repeated by Richter & LePage (2005), and resulted in the same conclusions. It is also worth noting that the assemblage of paleobotanical macrofossils is not specific within the Phanerozoic (Jahren & Sternberg 2002).

The strongest evidence that the Fossil Forest formed during the middle Eocene can be found within work by Eberle & Storer (1999); these researchers recovered three tooth fossils from float on a sandstone that directly overlies one fossiliferous stratum. The tooth fragments were identified as from the brontothere, a quadrupedal herbivore, which became extinct in the late Eocene (**Figure 6**). The fossils themselves are most similar to genera found elsewhere in the Arctic that correlate with the middle Eocene, thus cementing the ~45 Ma age for the Fossil Forest.

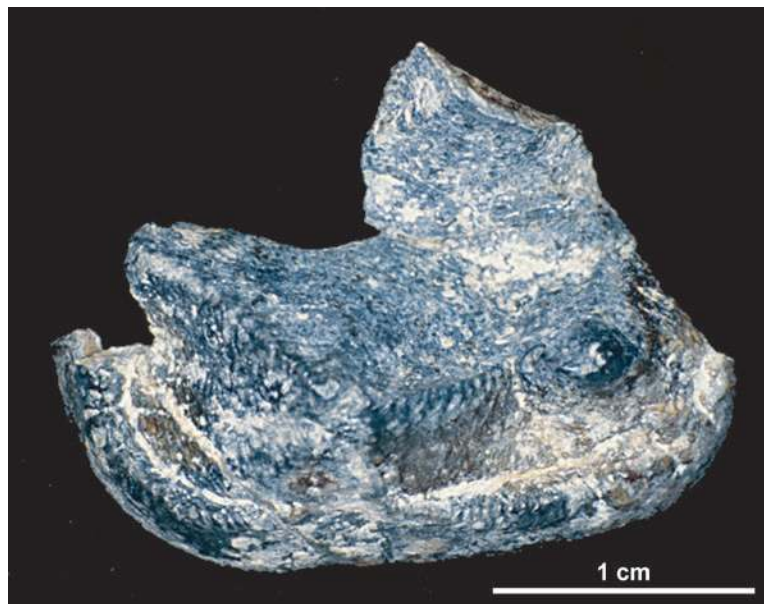


Figure 6

Cenozoic mammals, represented primarily by their teeth, are excellent index fossils for dating terrestrial strata because they are highly diagnostic, relatively abundant, and they evolved rapidly after the Cretaceous-Tertiary boundary. Teeth of large, rhinoceros-like brontotheres, including this incomplete premolar (CMN 51091) from the Fossil Forest, provide a time control for the Axel Heiberg Fossil Forest sediments. Specifically, the size and morphology of CMN 51091 and other brontothere fossils are most comparable to midlatitude brontotheres from the Uintan and Duchesnean North American Land Mammal Ages, correlative with middle Eocene time. Photo courtesy of J.J. Eberle.

FOSSIL ORGANISMS FOUND AT THE SITE

Metasequoia wood is, by far and away, the most abundant fossil within Fossil Forest strata (**Figure 7**); it is striking not only in its abundance, but also with respect to its exquisite preservation. The major anatomical features used to identify *Metasequoia* (at low resolution) include the presence of smooth-end walls of parenchyma (both ray and vertical) and the absence of resin canals, ray tracheids, and spiral thickenings (Obst et al. 1991). Extant *Metasequoia* can be found as moderate plantations within China and Japan (Williams et al. 2003a) and as single examples within botanical gardens and arboreta on many continents.

Excavations of macrofossils and palynomorphs within Fossil Forest strata revealed a lush and diverse Arctic ecosystem (**Figure 8**). **Table 1** catalogs the conifers (and the *Ginkgo* sp.) recovered from the site. Axel Heiberg Island was forested with fir, cypress,

Figure 7

Wood excavated from the Fossil Forest site, showing the exceptional preservation. (a) The largest trees found measured close to 3 m in diameter. (b) Juvenile trees were also found, sometimes still attached to the root bole. (c) Continuous lengths, sometimes several meters in length, were often found.





Figure 8

(a) The thick litter layer that blanketed the floor of the Fossil Forest, within which leaf, stem, cones, spores, and pollen are abundantly preserved. (b) Fossilized *Metasequoia* leaves. (c) Fossilized *Betula* leaves.

larch, redwood, spruce, pine, and hemlock trees. A survey of angiosperms (Table 2) reveals an understory and/or fringe vegetation containing maple, alder, birch, hickory, chestnut, beech, ash, holly, walnut, sweetgum, sycamore, oak, willow, and elm trees. As for small plants, honeysuckle and sumac were present, as were various reeds (Table 3).

Several species of ferns and mosses have been recovered (Table 4), either as paly-nomorphs or as preserved fronds. Based on the above, the Fossil Forest is envisioned as a mosaic of angiosperm, conifer, and fern communities in a continually changing floodplain environment (Liu & Basinger 2000, McIntyre 1991, Richter & LePage 2005).

Day (1991) extensively surveyed both fossil spores and propagules from the Buchanan Lake strata and identified at least three families of ascospores and at least five families of conidia; also present were nonsporic propagules. As part of a novel study, Labandeira et al. (2001) identified engravings in *Larix altoborealis* (larch) fossil wood as the work of *Dendroctonus*, a bark beetle.

The Fossil Forests of Axel Heiberg Island have allowed for several significant reinterpretations of plant and animal evolution. Most importantly, it was using these

Table 1 Conifer and Ginkgoaceae organisms found within middle Eocene sediments of the Fossil Forest of Axel Heiberg Island

Latin name	Common name	Fossil material	Reference
<i>Phylum Spermatophyta Gymnospermae and Coniferae</i>			
? <i>Abies</i> sp.	Fir	Palynomorph	McIntyre (1991)
<i>Cathaya</i> sp.	— ^a	Palynomorph	Liu & Basinger (2000)
<i>Chamaecyparis</i> sp.	False cypress	Leaf, plant fragment, twig	Basinger (1991), Greenwood & Basinger (1993), McIver & Basinger (1999)
?Cupressaceae ^b		Palynomorph	McIntyre (1991)
<i>Ginkgo</i> sp. ^c	Maidenhair	Leaf	Basinger (1991), McIver & Basinger (1999)
<i>Glyptostrobus</i> sp.	Swamp cypress	Leaf, plant fragment, palynomorph	Greenwood & Basinger (1993), McIntyre (1991), McIver & Basinger (1999), Richter & LePage (2005)
<i>Glyptostrobus nordenskioldii</i>	Swamp cypress	Leaf, twigs, cone	Basinger (1991)
<i>Larix</i> sp.	Larch	Cone, needle, palynomorph, twig	Basinger (1991), LePage & Basinger (1991), McIntyre (1991), McIver & Basinger (1999), Richter & LePage (2005)
<i>Larix altoborealis</i> sp. nov. ^d	Larch	Cone, needle, twig, wood	LePage & Basinger (1991)
<i>Metasequoia</i> sp.	Dawn redwood	Cone, leaf, stem, palynomorph, wood	Basinger (1991), Greenwood & Basinger (1993), McIntyre (1991), McIver & Basinger (1999), Richter & LePage (2005), Williams, et al. (2003)
<i>Metasequoia occidentalis</i>	Dawn redwood	Leaf, twigs, cone	Basinger (1991)
<i>Picea</i> spp.	Spruce	Cone, palynomorph, twig	Basinger (1991), Jagels et. al. (2001), McIntyre (1991), McIver & Basinger (1999)
<i>Picea beibergii</i> sp. nov.	Spruce	Cone	LePage (2001)
<i>Picea nansinii</i> sp. nov.	Spruce	Cone	LePage (2001)
<i>Picea palustris</i> sp. nov.	Spruce	Cone, leaf, twig	LePage (2001)
Family Pinaceae ^b		Palynomorphs	Richter & LePage (2005)
<i>Pinus</i> sp.	Pine	Cone, leaf fascicle, palynomorphs	Basinger (1991), McIntyre (1991), McIver & Basinger (1999)
<i>Pseudolarix</i>	Golden larch	Scale	Greenwood & Basinger (1993), McIver & Basinger (1999)
<i>Taiwania</i> sp.	—	Cone	McIver & Basinger (1999)
Family Taxodiaceae ^b		Leaf, stump, twig	Basinger (1991), Greenwood & Basinger (1993), McIver & Basinger (1999)
<i>Tsuga</i> sp.	Hemlock	Cone, palynomorph	McIntyre (1991), McIver & Basinger (1999), Richter & LePage (2005)
<i>Tsuga swedaeae</i> sp. nov.	Hemlock	Cone, twig	LePage (2002)

^aNo common name exists.

^bNot identified to genus.

^cNot a conifer.

^d"sp. nov." indicates a new species.

Table 2 Dicot angiosperms found within middle Eocene sediments of the Fossil Forest of Axel Heiberg Island

Latin name	Common name	Fossil material	Reference
<i>Phylum Spermatophyta Angiospermae (Dicotyledonae)</i>			
<i>Acer</i> sp.	Maple	Palynomorph	McIntyre (1991)
<i>Alnus</i> sp.	Alder	Fruit, leaf, palynomorph	Basinger (1991), Greenwood & Basinger (1993), McIntyre (1991), McIver & Basinger (1999), Richter & LePage (2005)
<i>Anacolisidites</i> sp. (cf. <i>A. reklarwensis</i> Elsik)	— ^a	Palynomorph	McIntyre (1991)
<i>Archeampelos</i> sp.	N.E. ^b	Leaf	McIver & Basinger (1999)
<i>Betula</i> spp.	Birch	Fruit, palynomorph	Basinger (1991), McIntyre (1991), McIver & Basinger (1999)
Family Betulaceae		Leaf	Basinger (1991), Greenwood & Basinger (1993), McIver & Basinger (1999)
<i>Carya</i> spp.	Hickory	Leaf, fruit, palynomorph	Basinger (1991), McIntyre (1991), McIver & Basinger (1991)
<i>Carya veripites</i>	Hickory	Palynomorph	McIntyre (1991)
<i>Carya viridifluminipites</i>	Hickory	Palynomorph	McIntyre (1991)
<i>Castanea</i> sp.	Chestnut	Palynomorph	McIntyre (1991)
<i>Cercidiphyllum</i> sp.	Katsura	Fruit, leaf, palynomorph	Basinger (1991), McIntyre (1991)
Family Cercidiphyllaceae		Fruit	McIver & Basinger (1999)
<i>Corylus</i> sp.	Hazel	Palynomorph	McIntyre (1991)
<i>Diervilla</i> sp.	—	Palynomorph	McIntyre (1991)
<i>Engelhardtia</i> sp. (cf. <i>E. chrysolepis</i>)	Chinquapin	Palynomorph	McIntyre (1991)
Family Ericaceae (<i>Ericipites</i> spp.)	N.E.	Palynomorph	McIntyre (1991)
<i>Fagus</i> sp.	Beech	Palynomorph	McIntyre (1991)
<i>Fraxinus</i> sp.	Ash	Palynomorph	McIntyre (1991)
<i>Gothanipollis</i> sp.	N.E.	Palynomorph	McIntyre (1991)
<i>Ilex</i> sp.	Holly	Palynomorph	McIntyre (1991)
<i>Intratrirporopollenites</i> sp. (cf. <i>Reevesia</i>)	No extant	Palynomorph	McIntyre (1991)
<i>Juglans</i> spp.	Walnut	Nut, palynomorph	McIntyre (1991), McIver & Basinger (1999)
Family Juglandaceae		Leaf	McIver & Basinger (1999)
<i>Liquidambar</i> sp.	Sweetgum	Palynomorph	McIntyre (1991)
<i>Lonicera</i> sp.	Honeysuckle	Palynomorph	McIntyre (1991)
Family Menispermaceae		Leaf	McIver & Basinger (1999)
<i>Myrica</i> sp.	Sweetgale	Palynomorph	McIntyre (1991)
<i>Nordenskiöldia borealis</i>	N.E.	Fruit, leaf	McIver & Basinger (1999)
<i>Nyssa</i> sp.	Tupelo	Fruit, palynomorph	McIntyre (1991), McIver & Basinger (1999)

(Continued)

Table 2 (Continued)

Latin name	Common name	Fossil material	Reference
<i>Nyssidium arcticum</i>	N.E.	Fruit, leaf	McIver & Basinger (1999)
<i>Pachysandra</i> sp.	—	Palynomorph	McIntyre (1991)
<i>Pistillipollenites mcgregorii</i> Rouse	N.E.	Palynomorph	McIntyre (1991)
? <i>Planera</i> sp.	—	Palynomorph	McIntyre (1991)
<i>Platanus</i>	Sycamore	Leaf	Basinger (1991), McIver & Basinger (1999)
<i>Pterocarya</i> spp.	—	Palynomorph	McIntyre (1991)
<i>Quercus</i> spp.	Oak	Leaf, palynomorph	Basinger (1991), McIntyre (1991), McIver & Basinger (1999)
<i>Rhus</i> sp.	Sumac	Leaf, palynomorph	McIntyre (1991), McIver & Basinger (1999)
Family Rosaceae		Palynomorph	McIntyre (1991)
<i>Salix</i> sp.	Willow	Palynomorph	McIntyre (1991)
<i>Tilia</i> sp. (<i>T. vespites</i> Wodehouse)	Linden	Palynomorph	McIntyre (1991)
<i>Treigonobalanus</i> sp.	—	Fruit	McIver & Basinger (1999)
<i>Tricolporopollenites kruschii</i>	N.E.	Palynomorph	McIntyre (1991)
<i>Ulmus</i> sp.	Elm	Leaf, palynomorph	McIntyre (1991), McIver & Basinger (1999)
<i>Ushia</i> sp.	—	Leaf	McIver & Basinger (1999)
? <i>Viburnum</i> sp. (cf. <i>V. cassinoides</i> L.)	—	Palynomorph	McIntyre (1991)

^aNo common name exists.

^bNone extant.

sediments that LePage & Basinger (1991b) described the earliest known occurrence of *Larix* (larch), which had previously been ambiguous prior to the Oligocene (LePage & Basinger 1995). Later, Jagels et al. (2001) provided the first definitive identification of fossil *Larix* wood through the identification of ray-tracheid bordered pits. The brontothere fragments (discussed above) discovered by Eberle & Storer (1999) constituted the northernmost record of Tertiary mammals (Eberle 2006).

Table 3 Monocot Angiosperms found within middle Eocene sediments of the Fossil Forest of Axel Heiberg Island

Latin name	Common name	Fossil material	Reference
<i>Phylum Spermatophyta</i> Angiospermae (Monocotyledonae)			
<i>Liliacidites</i> sp.	N.E. ^a	Palynomorph	McIntyre (1991)
<i>Monocolpopollenites</i> sp.	N.E.	Palynomorph	McIntyre (1991)
<i>Sparganium</i> sp.	Reed	Fruiting head, palynomorph	McIntyre (1991), McIver & Basinger (1999)

^aNone extant.

Table 4 Fern and fern-like organisms found within middle Eocene sediments of the Fossil Forest of Axel Heiberg Island

Latin name	Common name	Fossil material	Reference
<i>Phylum Pteridophyta</i>			
<i>Cryptogramma</i> sp.	Fern	Palynomorph	McIntyre (1991)
<i>Deltoidospora</i> spp.	N.E. ^a	Palynomorph	McIntyre (1991)
<i>Gleichenia</i> sp.	Fern	Palynomorph	McIntyre (1991)
<i>Laevigatosporites</i> spp.	N.E.	Palynomorph	McIntyre (1991)
<i>Lycopodium</i> spp.	Club moss	Palynomorph	McIntyre (1991)
Family Onoclea	Fern	Fronds, whole plant	Greenwood & Basinger (1993)
<i>Osmunda</i> spp.	Royal fern	Fronds, palynomorph	Greenwood & Basinger (1993), McIntyre (1991), McIver & Basinger (1999)
? <i>Polypodium</i> sp.	Fern	Palynomorph	McIntyre (1991)
<i>Radialisporis radiatus</i>	N.E.	Palynomorph	McIntyre (1991)

^aNone extant.

PALEOENVIRONMENT RECONSTRUCTIONS USING FOSSIL FOREST MATERIALS

Paleotemperature

Using disparate methods (**Table 5**), most workers have agreed that the middle Eocene forest of Axel Heiberg Island was subject to warm conditions, including MATs in excess of 12°C. The same studies have estimated mean cold-month temperatures in excess of 0°C, arguing against hard freeze events during the long, dark winters. Nearest-living-relative arguments (e.g., Basinger 1991, Francis 1991, McIntyre 1991) have emphasized a moist environment and lack of frost. The one exception to this interpretation resulted from Greenwood & Wing's (1995) multiple-regression model, which yielded significantly lower mean annual and cold-month mean temperatures for the Fossil Forest. Under this vision, mean temperatures were up to 5°C cooler than those suggested by other methods, including a climate-leaf analysis multivariate program (Wolfe 1994). The most recent paleotemperature determined for the site, based on the oxygen-isotope equilibration between environmental water and pedogenic carbonate, favors the warmer interpretation of the site (MAT = 13.2 ± 2.0°C) (Jahren & Sternberg 2003).

Atmospheric Carbon Dioxide Levels

No consensus exists as to the probable CO₂ content of the middle Eocene atmosphere (Royer 2006). Pearson & Palmer (2000) used the boron-isotope ratio of foraminifera to estimate the pH of surface-layer seawater, which was then used to reconstruct middle Eocene pCO₂ ≈ 2400 ppm (R ≈ 6.5×). Although boron isotopes have implied the highest levels of middle Eocene pCO₂, work by Lowenstein & Demicco (2006) estimated high pCO₂ levels (2200 ppm; R ≈ 6×) by examining assemblages of middle Eocene Na-carbonates and assuming that they had precipitated in contact with the

Table 5 Quantitative and qualitative estimates of paleotemperature made for the Eocene Arctic Fossil Forest

Temperature estimate (°C)			Qualitative description	Method	Reference
MAT ^a	MART ^b	CCM ^c			
13.2 ± 2.0				Oxygen isotope equilibration between environmental water and pedogenic carbonate	Jahren & Sternberg (2003)
13.7–17.2	—	3.3–8.6		CLAMP ^d	Wolfe (1994)
12–15	—	0–4	Mesothermal, moist, without severe winter frosts at low elevations Warm and moist environment Warm and equable, without appreciable winter frost Temperate to warm-temperate Temperate to warm-temperate with mild, wet winters and warm, moist summers	NLR ^e “based on current data” (probably informal NLR) NLR NLR NLR using pollen assemblages Analysis of paleosol features	Basinger et al. (1994) McIver & Basinger (1999) Francis (1991) Basinger (1991) McIntyre (1991) Tárnocai & Smith(1991)
9.3 ± 2.0	13.8 ± 5.1	−0.8 ± 3.6		MRM ^f	Greenwood & Wing (1995)

^aMean annual temperature.
^bMean annual range of temperature (only reported within Greenwood & Wing 1995).
^cCold-month mean.
^dClimate-leaf analysis multivariate program.
^eNearest-living-relative comparison.
^fMultiple-regression model.

paleoatmosphere. Studies invoking the isotopic composition of pedogenic carbonate through time as a paleobarometer of CO₂ have yielded the relatively high estimates of middle Eocene pCO₂ ≈1,950 ppm (R ≈ 2.6×) (Ekart et al. 1999). Studies of the carbon stable isotope composition of alkenones in deep sea cores implied a middle Eocene range in pCO₂ ≈1000–1500 ppm (R ≈ 2.7× to 4×) (Pagani et al. 2005). In contrast, the GEOCARB carbon-cycling model estimates middle Eocene pCO₂ to have been ≈700 ppm (R ≈ 2×; figure 13 of Berner & Kothavala 2001). Stomatal density measurements have resulted in yet more disparate estimates: Retallack (2001) determined a pCO₂ ≈ 1,000 ppm (R ≈ 2.7×; five-point running average based on **Figure 4b**), whereas Royer et al. (2001) used dissimilar methods to infer Eocene CO₂ levels to be near the same as that of today (R ≈ 1×). Owing to the myriad effects of elevated pCO₂ upon plant communities (and vice versa) (Schlesinger et al. 2006), the extent and composition of terrestrial forests during a given geological period cannot

reliably be used to speculate as to the level of CO₂ in the paleoatmosphere. For these reasons, the ambient CO₂ level of the middle Eocene Arctic forests remains a topic of active controversy.

Soil Methanogenesis

Another striking feature of the Axel Heiberg Fossil Forest is the exceptionally well-preserved paleosols, which exhibit distinct organic and mineral horizons as well as preserved litter layers and root mass (**Figure 9**). Tarnocai & Smith (1991) described podzolic, gleyed-podzolic, gleysolic, and organic paleosols, emphasizing the water-saturated, acidic, and chemically reducing organic soil environment that existed within the Fossil Forest during the middle Eocene. They emphasized the integration of these soils into a floodplain environment with mild, wet winters and warm, moist summers. Some Fossil Forest paleosols exhibit enigmatic white layers that Tarnocai et al. (1991) investigated via X-ray diffraction and particle-size analyses. Much of the white material was revealed to be quartz with platy morphology; Tarnocai et al. (1991) proposed that this comprised the concentrated remains of opal phytoliths.

Within some of these paleosols is tree fossil material that has been diagenetically replaced with pedogenic carbonate. This replacement is notable, not only because it resulted soon after burial, given the lack of physical deformation of the macrofossil, but also because organic matter has been replaced at the cellular scale, preserving the tracheid morphology of the original tissue (**Figure 10c**). These unusual secondary mineral deposits led Jähren et al. (2004) to use the carbon-isotope composition of organic carbon compared to carbonate to investigate carbon-cycling processes within the soils of the Fossil Forest. The fossil carbonate exhibited strikingly high $\delta^{13}\text{C}$

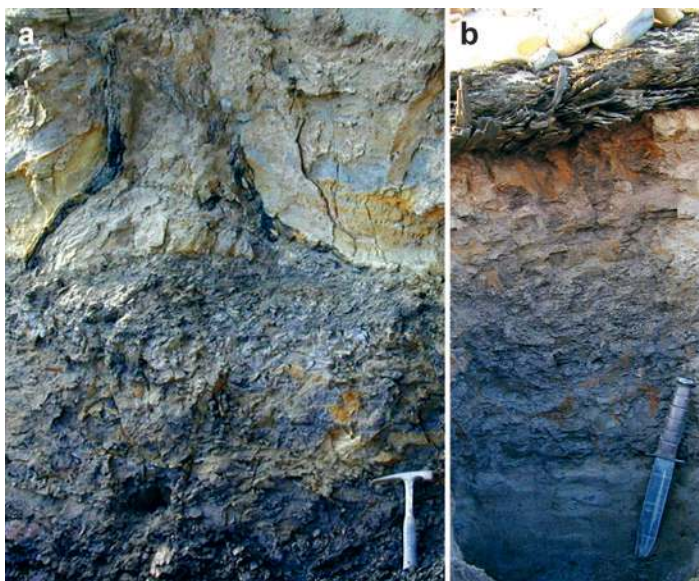


Figure 9

Exquisite paleosols are preserved within the Fossil Forest, some still bearing the outline of trees that grew within the soil (a), others exhibiting clear O, A, and B horizons (b).

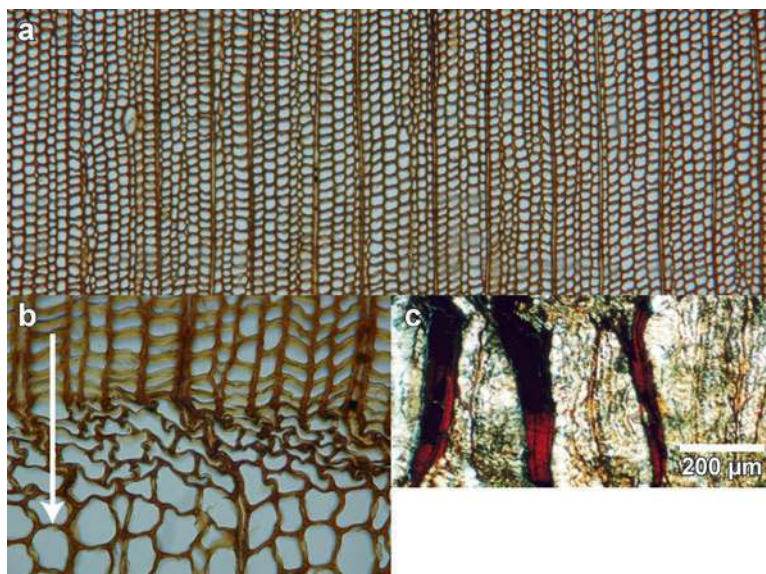
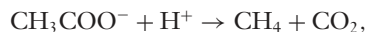


Figure 10

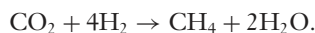
Light-microscope images of the cellular structure of fossil wood excavated from Axel Heiberg Island. (a) Late wood, with individual cells $\sim 25 \mu\text{m}$ in diameter and abundant ray cells. (b) The transition of late wood into early wood, with arrow indicating the direction of growth. Early wood cells measure $\sim 40 \mu\text{m}$ in diameter and are often compacted owing to burial. (c) Wood samples within which organic carbon (*dark areas*) has been partially replaced by carbonate (*light areas*) while preserving the wood microstructure.

values ($+4.0\text{‰}$ to $+7.4\text{‰}$), consistent with the idea that methanogenesis resulted in a ^{13}C -enriched CO_2 pool that equilibrated with soil water and gave rise to unusually ^{13}C -enriched pedogenic carbonate $\delta^{13}\text{C}$ values.

Other workers have reported conspicuously high $\delta^{13}\text{C}$ values within Mesozoic pedogenic carbonate and linked them with methanogenesis (e.g., Ludvigson et al. 1998; Ufnar et al. 2002, 2004). The gray colors, silty textures, and coarse mottling observed in Fossil Forest paleosols (**Figure 9**) are features associated with hydromorphic soils featuring low pH, low O_2 levels, and generally reducing conditions (Fastovsky & McSweeney 1987). Microsites within these soils may have alternately favored both the precipitation of carbonate and carbon cycling within microbial communities (Rask & Schoenau 1993). Biogenic methane production occurs in generally reducing terrestrial environments via two primary pathways: acetate fermentation:



and the reduction of CO_2 :



Consideration of the fractionation factors (α) previously determined for these pathways (Gelwicks et al. 1994, Sugimoto & Wada 1993) and the isotopic difference between organic carbon and carbonate in the samples revealed that >80% of the carbon precipitated as carbonate resulted from the equilibration of CO₂ produced via acetate fermentation, in accordance with values observed for modern ecosystems (Hornibrook et al. 2000, Whiticar et al. 1986). The abundant preservation and partial decomposition of deciduous plant tissue would comprise a huge pool of acetate available for reduction within the Eocene Arctic forests: Annual leaf contributions have been estimated to be 320 g m⁻² year⁻¹ within the Fossil Forest (Williams et al. 2003a,b). Given the carbon-cycling budgets of modern acetate-rich ecosystems (Küsel & Drake 1999), these values suggest that the maximum CH₄ release to the atmosphere due to these processes would have been $\approx 24 \text{ g C}_{\text{CH}_4} \text{ m}^{-2} \text{ year}^{-1}$ (Jahren et al. 2004). Because it is a powerful greenhouse gas (Lashof & Ahuja 1990), methane might have been an especially important component of the middle Eocene atmosphere, helping to maintain the elevated temperatures described above, particularly under a scenario featuring modest CO₂ levels (e.g., Royer et al. 2001).

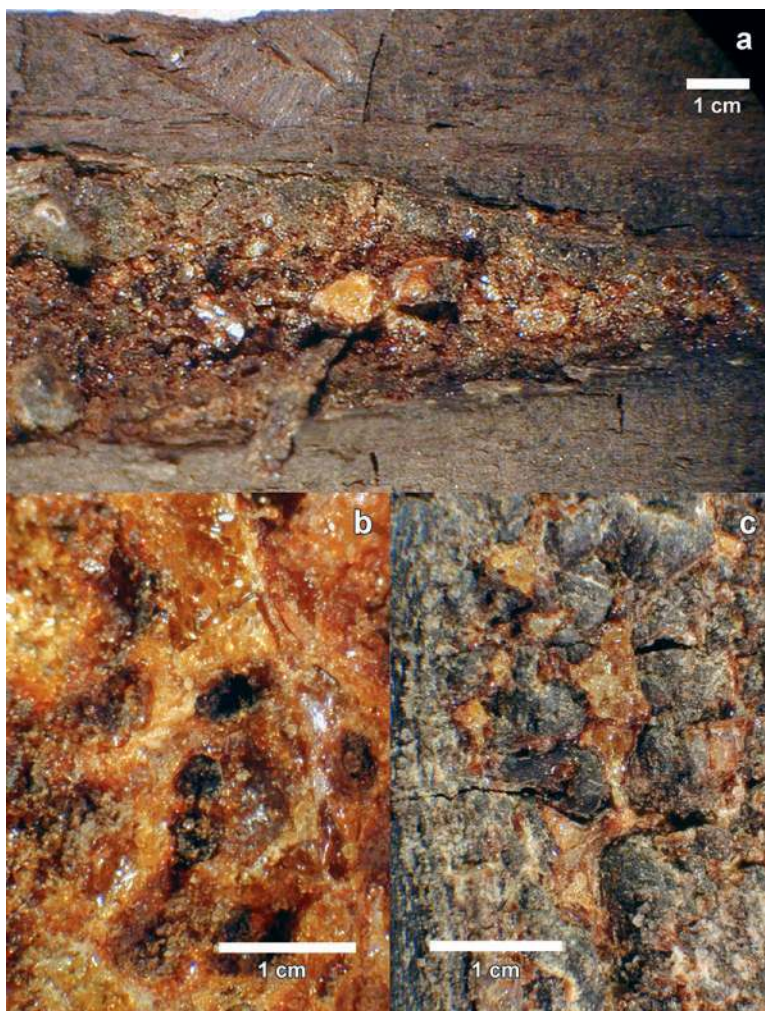
Lack of Arctic Ice

Obst et al. (1991) performed the first chemical characterization of the organic component of Axel Heiberg fossils, which showed fossil wood to be rich in lignin (up to 80% lignin by mass). However, the same study postulated that fossilized gymnosperms had undergone extensive carbohydrate degradation with near complete removal of hemicelluloses. This was later refuted by multiple studies that identified, purified, and isolated both hemicellulose and α -cellulose (Jahren & Sternberg 2002, 2003, 2007). Yang et al. (2005) investigated the biomolecular preservational status of *Metasequoia* leaves and wood in Tertiary fossils using a comparative pyrolysis approach. They found that pyrolysates from middle Eocene Axel Heiberg *Metasequoia* wood were dominated by lignin-derived phenol compounds and proposed that the presence of structural polyphenolic compounds as initial decay products, such as tannins, provided resistance to further microbial and fungal degradation by binding to cellulose and other biomolecules. This may be a possible explanation for the exceptional preservation of the Fossil Forest paleovegetation.

A large amount of fossilized resin can be found within the sediments and the litter layers of the Fossil Forest (**Figure 11**), perhaps copiously produced by *Pseudolarix* as a defense compound (Anderson & LePage 1995). In addition, the abundance of higher-plant waxes gives rise to high concentrations of lipids, particularly odd-carbon-numbered *n*-alkanes. In particular, Yang et al. (2005) stated that the C₂₉ predominance within Fossil Forest litter layers reflects the whole-leaf signature of *Metasequoia* spp., as opposed to leaf surfaces alone where C₂₅ predominates. Jahren et al. (2007) isolated lipids from 19 lignite layers of the Buchanan Lake Formation and analyzed *n*-alkane biomarkers for hydrogen-stable isotopes to reconstruct the hydrogen-isotope composition (δD) of the precipitation value of paleoenvironmental water above the Arctic Circle during the middle Eocene. Comparatively few *n*-alkanes with a chain length <C₂₀ were found, indicating that diagenetic and catagenetic alteration was minimal,

Figure 11

Fossilized resin preserved within sediment (a), wood (b), and litter (c) from the Fossil Forest.



consistent with the exceedingly mild thermal history of the formation (Ricketts 1991). Using the methods detailed within Byrne (2005), the average δD value of n -alkanes in each stratigraphic layer ranged from -284.6‰ to -252.5‰ .

During the synthesis of lipids, most hydrogen is ultimately derived from cell water (Chikaraishi & Naraoka 2003, Sessions et al. 2002). The most applicable fractionation factor for the Fossil Forest ecosystem is found within Chikaraishi et al.'s (2004) work, which gives

$$\alpha = \frac{R_{n\text{-alkane}}}{R_{\text{environmental water}}} = 0.884 \left(R = D/H \right),$$

specifically for conifers growing under high relative humidity. Using $\alpha_{\text{Chikaraishi}}$, values of $\delta D_{\text{environmental water}}$ can be reconstructed in the following way:

$$\delta D_{\text{environmental water}} [\text{‰}] = \frac{[\delta D_{n\text{-alkane}} - (\alpha - 1) \cdot 1000]}{\alpha}.$$

Using the above, calculated $\delta D_{\text{environmental water}}$ ranged from -191‰ to -154‰ . These values overlap with the range of $\delta D_{\text{environmental water}}$ estimates made from fossil cellulose $\delta^{18}\text{O}$ (-183‰ to -110‰) (Jahren & Sternberg 2003). The above reconstructions of Fossil Forest $\delta D_{\text{environmental water}}$ value are considerably higher than values obtained from the site for modern soil water (average = -200‰), stream water (average = -205‰), and ice pack (average = -208‰). Today, the δD value of precipitation in the Axel Heiberg locale is approximately -220‰ (Bowen & Ravenaugh 2003) or $-213 \pm 7\text{‰}$ (Glob. Netw. Isot. Precip. 2001, IAEA/WMO 2006, Global Network of Isotopes in Precipitation. The GNIP Database. Accessible at: <http://isohis.iaea.org>), as measured at Resolute Bay (74.72°N and -94.98°E).

This difference between the stable-isotope values of modern Arctic environmental water and those of middle Eocene environmental water imply a wholly different water cycle within northern high latitudes, relative to today. To illustrate, the Bowen-Wilkinson equation (Bowen & Wilkinson 2002) can be used to calculate the expected oxygen-isotope ratios of precipitation ($\delta^{18}\text{O}$) at the latitudes (LAT) and minimum altitudes (ALT) of modern snow and ice fields:

$$\delta^{18}\text{O} [\text{‰}] = (-0.0051 \times \text{LAT}^2) + (0.1805 \times \text{LAT}) + (-0.002 \times \text{ALT}) - 5.247.$$

The δD value of precipitation can then be calculated using the linear relationship given by the global meteoric water line first established by Craig (1961):

$$\delta D [\text{‰}] = m \delta^{18}\text{O} + 10,$$

using a slope of $m = 9.5$ (see below) (Jahren & Sternberg 2003).

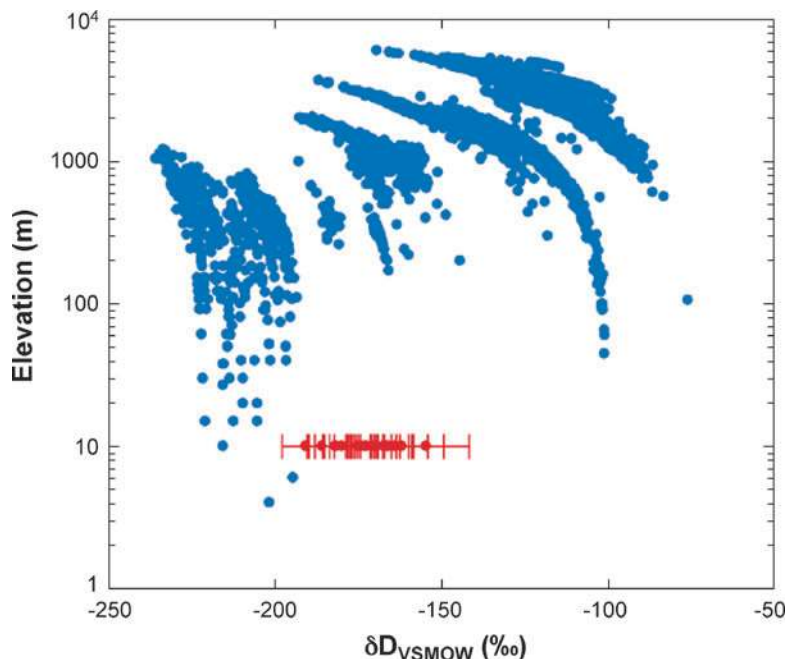
The relationship between the calculated δD value of precipitation (blue data) and the minimum altitude of present-day snow and ice fields is depicted in **Figure 12**; the red data within represent the reconstructed δD values of environmental water for the Arctic Eocene Fossil Forest based on *n*-alkanes (Jahren et al. 2007). The δD values of Eocene water plot within an area of the graph that shows no overlap with the δD values of modern ice masses within the Northern Hemisphere. On the basis of the general similarity between Eocene and modern tectonic plate configurations, this lack of overlap implies a middle Eocene Arctic lacking in snowfall and certainly lacking sufficient accumulation for an ice pack or a glacier. Taken in conjunction with other stable-isotope data, the δD values of *n*-alkanes within the lignites of the Fossil Forest are consistent with a spatially equable climate system, without extremes of temperature at the poles; these data also preclude the extensive buildup of ice and snow, even through three months of darkness.

Relative Humidity

The exquisite preservation of tree fossil material on Axel Heiberg Island makes possible the implementation of stable-isotope paleoclimatological techniques (reviewed

Figure 12

The hydrogen-isotope composition of environmental water as predicted from *n*-alkanes within resin isolated from fossil litter layers (*red data*). These values show no overlap with the hydrogen-isotope composition of ice masses between 0 and 90°N latitude (*blue data*). All values are presented against minimum elevation; *n*-alkane-based predictions are shown with associated standard deviation.



in McCarroll & Loader 2004) usually relegated to Quaternary substrates. For example, workers have obtained $\delta^{18}\text{O}$ and δD values from cellulose and cellulose nitrate, respectively, using tree fossils from Axel Heiberg Island. Just as with modern wood, fossil wood was removed of lipids, lignin, and hemicellulose to obtain pure α -cellulose (Sternberg 1989); oxygen in cellulose was converted into CO_2 for $\delta^{18}\text{O}$ analysis via reaction with HgCl_2 (Sauer & Sternberg 1994). A 200-mg portion of α -cellulose was subjected to standard nitration procedure; water produced by the combustion of cellulose nitrate was recovered as H_2 (Sternberg 1989). This was possible for both bulk fossil wood samples (Jahren & Sternberg 2003), as well as fossil rings, including intraseasonal subsampling (Jahren & Sternberg 2007).

Middle Eocene fossil wood used for analysis was identified as *Metasequoia glyptostroboides* and often represented small subsamples from the large wood samples excavated by Williams et al. (2003b). This identification was based on the gross anatomy and branching pattern in stems, as well as the abundance of *Metasequoia* in Fossil Forest litter layers. Regarding the wood fossil rings that were subsampled to assess intraseasonal variations in paleoenvironment (**Figure 10**), all fossils were identified as of either *Metasequoia* or *Glyptostrobus* genus (G. Visscher, personal communication). This identification was based on the presence or absence of microscopic resin canals in the form of fusiform rays (Jagels et al. 2001, 2003).

Because the ultimate oxygen and hydrogen isotopic composition of cellulose in tree rings is controlled by processes internal and external to the tree, $\delta^{18}\text{O}$ and δD values from cellulose and cellulose nitrate, respectively, can be used to interpret environmental water cycling. Processes external to the tree govern the isotopic composition

of environmental water in the ecosystem and contribute to the isotopic labeling of cellulose contained in nonphotosynthetic tissues such as tree trunks and roots, resulting in the heterotrophic component of the plant's isotopic signature. In addition, the plant's internal response to environmental humidity governs the isotopic composition of leaf water and contributes to the isotopic labeling of carbohydrates at the site of photosynthesis, resulting in the autotrophic component of the plant's isotopic signature. The final isotopic value (δ = either δD or $\delta^{18}\text{O}$) of tree-ring cellulose can therefore be described by (Roden & Ehleringer 1999)

$$\delta_{\text{cellulose}} = f(\delta_{\text{heterotrophic}}) + (1 - f)(\delta_{\text{autotrophic}}),$$

which separates the heterotrophic and autotrophic contribution of ecosystem processes into fractional (f) contributions to the ultimate cellulose composition.

Previous measurements on three species of trees indicated that 32% of hydrogen and 42% of oxygen atoms in cellulose have undergone exchange with stem water during cellulose synthesis; the remainder retained the isotopic signal acquired during isotopic exchange with leaf water (Roden & Ehleringer 1999, Roden et al. 2000). The net biochemical fractionation between cellulose and water during heterotrophic synthesis of cellulose was observed to be 158‰ for δD and 30‰ for $\delta^{18}\text{O}$ (Luo & Sternberg 1992; Sternberg et al. 1986, 2006; Yakir & DeNiro 1990). Experiments with *Lemna gibba* have indicated that the total change in isotopic composition due to autotrophic processes between leaf water and carbohydrate intermediates during cellulose synthesis is -171‰ for δD and 27‰ for $\delta^{18}\text{O}$ (Yakir & DeNiro 1990). These findings lead to the relationship

$$\delta_{\text{cellulose}} = f(\delta_{\text{stem water}} + \epsilon_{\text{heterotrophic}}) + (1 - f)(\delta_{\text{leaf water}} + \epsilon_{\text{autotrophic}}),$$

which recasts the heterotrophic contribution as the composition of stem water modified by the net heterotrophic biochemical isotopic fractionation between stem water and carbohydrate intermediates during cellulose synthesis ($\epsilon_{\text{heterotrophic}}$), and also recasts the autotrophic contribution as the composition of leaf water modified by the net autotrophic biochemical isotopic fractionation between leaf water and carbohydrate intermediates during cellulose synthesis ($\epsilon_{\text{autotrophic}}$).

The isotopic composition of leaf water undergoing transpiration is described by (as discussed in Yakir & Sternberg 2000)

$$\delta_{\text{leaf water}} = \delta_{\text{stem water}} + E_{\text{eq}} + E_{\text{k}} + (\delta_{\text{vapor}} - \delta_{\text{stem water}} - E_{\text{k}})(e_{\text{a}}/e_{\text{l}}),$$

where δ_{vapor} is the isotopic composition of water vapor in the atmosphere, E_{eq} and E_{k} are the respective equilibrium and kinetic isotopic fractionations between liquid water and the vapor generated during evaporation, and e_{a} and e_{l} represent atmospheric vapor pressure and the vapor pressure inside the leaf, respectively. Environmental water has been shown to enter the plant passively without isotopic fractionation (i.e., $\delta_{\text{stem water}} = \delta_{\text{environmental water}}$) (White 1988). Assuming that atmospheric water vapor is in isotopic equilibrium with environmental water, the isotopic composition of atmospheric water

vapor can be expressed as

$$\delta_{\text{vapor}} = \delta_{\text{stem water}} - E_{\text{eq.}}$$

In addition, assuming that the temperature of the leaf is nearly equal to that of the atmosphere allows for the vapor pressure ratio e_a/e_1 to be approximated by fractional humidity (b):

$$\delta_{\text{leaf water}} = \delta_{\text{stem water}} + (E_{\text{eq}} + E_k)(1 - b).$$

One can then write

$$\begin{aligned} \delta_{\text{cellulose}} = & f(\delta_{\text{stem water}} + \varepsilon_{\text{heterotrophic}}) \\ & + (1 - f)[\delta_{\text{stem water}} + (E_{\text{eq}} + E_k)(1 - b) + \varepsilon_{\text{autotrophic}}]. \end{aligned}$$

Widespread observation of the linear relationship $\delta D = m\delta^{18}\text{O} + b$ in environmental water (Craig 1961) allows one to solve for fractional humidity (b) during the Eocene using the isotopic composition of fossil cellulose. Specification for $\delta^{18}\text{O}$ and δD values yields

$$\begin{aligned} \delta D_{\text{cellulose}} = & m\delta^{18}\text{O}_{\text{environmental water}} + b + f_H \varepsilon_{\text{heterotrophic-H}} \\ & + (1 - f_H)[(E_{\text{eq-H}} + E_{k-H})(1 - b) + \varepsilon_{\text{autotrophic-H}}] \end{aligned}$$

and

$$\begin{aligned} \delta^{18}\text{O}_{\text{cellulose}} = & \delta^{18}\text{O}_{\text{environmental water}} + (f_O \varepsilon_{\text{heterotrophic-O}}) \\ & + (1 - f_O)[(E_{\text{eq-O}} + E_{k-O})(1 - b) + \varepsilon_{\text{autotrophic-O}}], \end{aligned}$$

where m is the slope and b is the y -intercept of the linear relationship between environmental $\delta^{18}\text{O}$ and δD values, and the subscripts H and O specify the relevant isotope. Given the known and fixed terms describing the isotopic linear relationship of environmental water, and the biochemical and kinetic fractionations for both isotopes, it is possible to solve the last two equations simultaneously for humidity and $\delta^{18}\text{O}_{\text{environmental water}}$ on Axel Heiberg Island during the middle Eocene. Because the solution is highly sensitive to the value of the slope (m) used to characterize the relationship between environmental $\delta^{18}\text{O}$ and δD values, and because Jahren & Sternberg (2003) found that fossil cellulose from Axel Heiberg Island exhibited a strikingly high slope ($m = 9.5$), this is the value of m used in calculating Eocene humidity.

Using the above methods, Jahren & Sternberg (2003) calculated an average growing-season-relative humidity of $\sim 67\%$ within the middle Eocene Arctic forests. Assuming $\text{MAT} \approx 13.2 \pm 2.0^\circ\text{C}$ (Table 5) implies a climate similar to that experienced within the Pacific Northwest today. Intraseasonal subsampling of growth rings within fossil wood revealed distinct patterns in $\delta^{18}\text{O}$ and δD values, which allowed for the calculation of changes in relative humidity during the growing season (Jahren & Sternberg 2007). Intraseasonal subsampling of fossil tree rings from Axel Heiberg Island revealed increases in relative humidity and reflected an end-of-season humidity regime of between 90% and 100% (Figure 13). Such massive increases in relative humidity would be expected from an ecosystem that experienced high annual rates

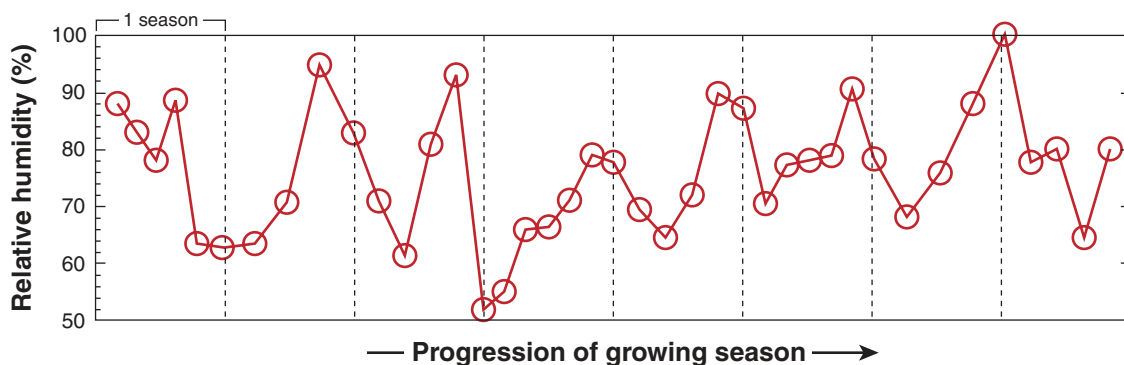


Figure 13

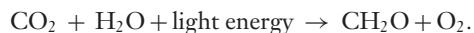
Patterns in changing relative humidity during the growing season, as calculated from the oxygen- and hydrogen-isotope composition of fossil cellulose, sampled within rings of fossilized *Metasequoia*. Intraseasonal variability shows a steady increase in relative humidity to very high levels (approaching 100%) by the end of the growing season.

of evapotranspiration associated with explosive deciduous growth (Mora & Jahren 2003).

Application of the Clausius-Clapeyron equation in conjunction with the ideal gas law allows for the calculation of the actual vapor pressure of water in the atmosphere, as well as its total mass in a given volume. Present-day high-Arctic ecosystems have actual vapor pressure of 4.1 mm Hg during the growing season (4.3 g H₂O per m³ of atmosphere). Given the relative humidity and temperature estimates discussed here, the Arctic middle Eocene entailed an actual paleo-vapor pressure of $\sim 8.2 \pm 0.9$ mm Hg on Axel Heiberg Island (8.3 ± 0.9 g H₂O per m³ of atmosphere). This value is approximately double the atmospheric water content seen in the Arctic today. This increased atmospheric water content would have contributed to a greenhouse effect during the middle Eocene, thus increasing atmospheric mixing and delivering water vapor to higher levels of the Arctic atmosphere. Although such a water-vapor feedback would not have caused middle-Eocene-warm temperatures, it would have helped maintain the warmth, particularly through the dark polar winters.

Carbon Loss through Respiration

Photosynthesis is the basic process by which plants convert CO₂ into carbohydrate, using light energy as an energy source:



Photosynthesis by conifers is always accompanied by the process of photorespiration, which consumes oxygen and releases CO₂ in the presence of light. Photorespiration reduces the efficiency of photosynthesis by wasting the activity of the photoenzyme RuBisCO, resulting in only one molecule of 3-phosphoglycerate and thus reducing

net carbon fixation during metabolism. Dark respiration is a similar process that occurs during the absence of light, again resulting in carbon leakage from the plant organism. Because of the continuously dark three-month winters implied by the geographical location of the Fossil Forest during the Eocene (**Figure 1** and **Figure 5**), researchers have hypothesized that deciduousness in Arctic *Metasequoia* of the middle Eocene was the primary strategy for eliminating carbon loss due to unabating dark respiration during the winter. However, greenhouse experiments have shown that the quantity of carbon lost annually by shedding a deciduous canopy is significantly greater than that lost by evergreen trees through wintertime respiration and leaf-litter production (Royer & Beerling 2003).

By intraseasonally microsampling tree rings, Helle & Schleser (2004) repeatedly observed a distinct annual pattern in the $\delta^{13}\text{C}$ value of modern wood from broadleaf species. These authors interpreted the trends they saw: (a) At the beginning of the growing season, a systematic increase in $\delta^{13}\text{C}$ value was due to the mobilization of stored carbon with inherently high isotopic value; (b) during the growing season, a systematic decrease in $\delta^{13}\text{C}$ value was due to the steadily increasing incorporation of recently fixed carbon with inherently low isotopic value; and (c) a systematic increase in $\delta^{13}\text{C}$ value during the late season was due to respiration, which preferentially removes light carbon from the organism.

Microsampling of Axel Heiberg wood at high resolution (Jahren & Sternberg 2007) revealed the patterns seen in **Figure 14**. On average, the $\delta^{13}\text{C}$ values of fossil

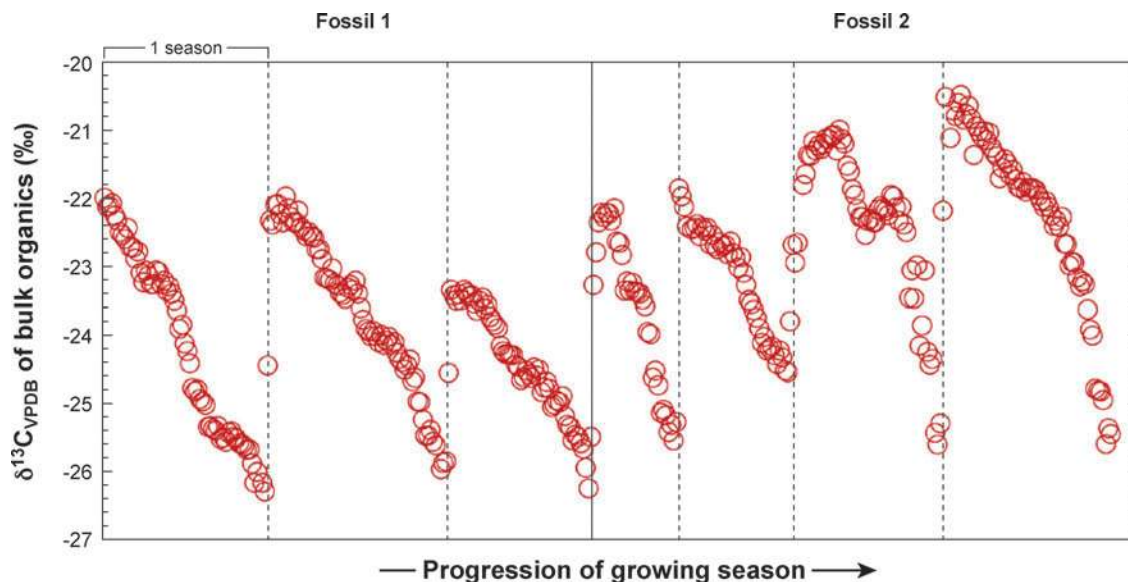


Figure 14

Observed patterns in the carbon-isotope signature of fossil wood, sampled at high resolution. Dashed lines indicate the division between adjacent rings (the late-wood/early-wood boundary); the solid line separates the two fossils analyzed. Each ring was sampled into at least 50 consecutive subsamples.

rings decreased by approximately 4‰ to 5.5‰ during the course of the growing season; this decreasing trend was apparent for every fossil ring analyzed. This pattern indicates that synthesized wood reflects a switchover from stored carbon to actively photosynthesized carbon during the growing season of these Arctic fossils. These results accentuate the deciduous habit of these trees; conifer trees show a different pattern in $\delta^{13}\text{C}$ value as microsampled within tree rings. In particular, Barbour et al. (2002) showed that, within conifers growing at middle-to-high latitudes, lowest $\delta^{13}\text{C}$ values occurred when temperatures were highest, relative humidity was lowest, and water stress was most intense. We are confronted with a truly unique ecosystem: that of extensive deciduous conifer forests that persist through polar light-regimes during summer and winter. The short duration of transitional seasons (**Figure 14**) may have led to a rapid shutdown period during the shedding of leaf tissue.

THE EMERGENT VISION OF THE SITE

The studies discussed here leave us with a unique vision of a middle Eocene ecosystem, thriving above the Arctic Circle. We imagine lush conifer forests, dominated by deciduous *Metasequoia*, complemented by a diverse understory of flowering trees and shrubs. Ferns and fungi inhabited the water-saturated soils, from which significant methanogenesis followed acetate reduction. Temperatures were warm, rarely if ever below freezing, and greater than 12°C as an annual average; we do not believe there was an ice pack in this polar region. Although we do not know the exact CO_2 level, we believe it was not lower than that of today. Relative humidity levels were high, particularly at the end of the growing season, implying a rain forest environment. Finally, the explosive deciduous growth of these conifer forests resulted in a thick organic litter layer that provided shelter for invertebrate and vertebrate animals.

SUMMARY POINTS

1. During the middle Eocene (~45 Ma), extensive forested landmasses located above the Arctic Circle were subject to three months of total darkness and three months of continuous light each year.
2. Paleobotanical excavations of Axel Heiberg Island, in Arctic Canada, have revealed lush deciduous conifer forests of middle Eocene age, dominated by *Metasequoia*.
3. Macrofossil and palynomorph identification revealed the presence of fir, cypress, larch, redwood, spruce, pine, and hemlock trees, with an understory containing maple, alder, birch, hickory, chestnut, beech, ash, holly, walnut, sweetgum, sycamore, oak, willow, and elm trees.
4. Paleosols from the site suggest water-saturated, acidic, and chemically reducing organic soil environments within the Fossil Forest, conducive to methanogenesis via acetate reduction.

5. Diverse methods have indicated that MATs exceeded 12°C within the Fossil Forest, and that heavy frosts did not occur. No consensus exists as to the pCO₂ levels during the time.
6. Stable-isotope analyses of extracted cellulose and *n*-alkanes imply the absence of arctic ice and high relative humidity, often approaching 100% toward the end of the growing season.
7. Intraseasonal carbon-isotope analyses of *Metasequoia* tree rings show a clearly deciduous pattern of carbon storage and photosynthetic carbon assimilation, including efficient senescence prior to the long, dark polar winter.

FUTURE ISSUES

1. An unequivocal estimate of middle Eocene CO₂, confirmed via multiple techniques, is badly needed in order to more fully understand the carbon cycle of the period and related greenhouse conditions.
2. A reliable way of estimating the total amount of geologic time contained within the stratigraphic lignites of the Fossil Forest would allow for high-resolution studies of changing environments, particularly within shifting understory communities.
3. Fieldwork on other middle Eocene sites will help elucidate the general versus specific nature of the Axel Heiberg Fossil Forest.

ACKNOWLEDGMENTS

This work could not have been completed without the field and laboratory expertise of W.M. Hagopian. I thank L.S.L. Sternberg and R.E. Summons for helpful conversations and B.A. LePage and J.F. Basinger for advice regarding the field site.

LITERATURE CITED

- Anderson KB, LePage BA. 1995. Analysis of fossil resins from Axel Heiberg Island, Canadian Arctic. In *Amber, Resinite, and Fossil Resins*, ed. KB Anderson, JC Crelling, pp. 170–92. Washington, DC: Am. Chem. Soc.
- Barbour MM, Walcroft AS, Farquhar GD. 2002. Seasonal variation in δ¹³C and δ¹⁸O of cellulose from growth rings of *Pinus radiata*. *Plant Cell Environ.* 25:1483–99
- Basinger JF. 1991. The fossil forests of the Buchanan Lake Formation (early Tertiary), Axel Heiberg Island, Canadian Arctic Archipelago: preliminary floristics and paleoclimate. In *Tertiary Fossil Forests of the Geodetic Hills, Axel Heiberg Island, Arctic Archipelago*, ed. RL Christie, NJ McMillan, pp. 39–65. Ottawa: Geol. Surv. Can.

- Basinger JF, McIver EE, LePage BA. 1988. The fossil forests of Axel Heiberg Island. *Musk Ox J.* 36:50–55
- Berner RA, Kothavala Z. 2001. GEOCARB III; a revised model of atmospheric CO₂ over Phanerozoic time. *Am. J. Sci.* 301:182–204
- Bigras C, Bilz M, Grattan DW, Gruchy C. 1995. Erosion of the Geodetic Hills Fossil Forest, Axel Heiberg Island, Northwest Territories. *Arctic* 48:942–53
- Bowen GJ, Ravenaugh J. 2003. Interpolating the isotopic composition of modern meteoric precipitation. *Water Resour. Res.* 39:1299, doi: 10.1029/2003WR002086
- Bowen GJ, Wilkinson BH. 2002. Spatial distribution of $\delta^{18}\text{O}$ in meteoric precipitation. *Geology* 30:315–18
- Byrne M. 2005. *A stable isotope stratigraphy of the Axel Heiberg Fossil Forest and its application to Eocene climate*. MS thesis. Mass. Inst. Tech. 107 pp.
- Chikaraishi Y, Naraoka H. 2003. Compound-specific δD - $\delta^{13}\text{C}$ analyses of *n*-alkanes extracted from terrestrial and aquatic plants. *Phytochemistry* 63:361–71
- Chikaraishi Y, Naraoka H, Poulson SR. 2004. Carbon and hydrogen isotopic fractionation during lipid biosynthesis in a higher plant (*Cryptomeria japonica*). *Phytochemistry* 65:323–30
- Craig H. 1961. Isotopic variations in meteoric waters. *Science* 133:1702–3
- Dalai TK, Ravizza GE, Peucker-Ehrenbrink B. 2006. The Late Eocene Os-187/Os-188 excursion: chemostratigraphy, cosmic dust flux and the Early Oligocene glaciation. *Earth Planet. Sci. Lett.* 241:477–92
- Day RG. 1991. An overview of fossil fungi in the Geodetic Hills Fossil Forest, Axel Heiberg Island, N.W.T. In *Tertiary Fossil Forests of the Geodetic Hills, Axel Heiberg Island, Arctic Archipelago*, ed. RL Christie, NJ McMillan, pp. 99–121. Ottawa: Geol. Surv. Can.
- DeConto RM, Pollard D. 2003. Rapid Cenozoic glaciation of Antarctica induced by declining atmospheric CO₂. *Nature* 421:245–49
- Eberle JJ. 2006. Early Eocene Brontotheriidae (Perissodactyla) from the Eureka Sound Group, Ellesmere Island, Canadian High Arctic—implications for brontothere origins and high-latitude dispersal. *J. Vertebr. Paleontol.* 26:381–86
- Eberle JJ, Storer JE. 1999. Northernmost record of brontotheres, Axel Heiberg Island, Canada—implications for age of the Buchanan Lake Formation and brontothere paleobiology. *J. Paleontol.* 73:979–83
- Ekat DD, Cerling TE, Montañez IP, Tabor NJ. 1999. A 400 million year carbon isotope record of pedogenic carbonate: implications for paleoatmospheric carbon dioxide. *Am. J. Sci.* 299:805–27
- Fastovsky DE, McSweeney K. 1987. Paleosols spanning the Cretaceous-Paleogene transition, eastern Montana and western North Dakota. *Geol. Soc. Am. Bull.* 99:66–77
- Forsythe WC, Rykiel EJ, Stahl RS, Wu H, Schoolfield RM. 1995. A model comparison for daylength as a function of latitude and day of year. *Ecol. Model.* 80:87–95
- Francis JE. 1991. The dynamics of polar fossil forests: Tertiary fossil forests of Axel Heiberg Island, Canadian Arctic Archipelago. In *Tertiary Fossil Forests of the Geodetic Hills, Axel Heiberg Island, Arctic Archipelago*, ed. RL Christie, NJ McMillan, pp. 29–38. Ottawa: Geol. Surv. Can.

- Gelwicks JT, Risatti JB, Hayes JM. 1994. Carbon isotope effects associated with aceticlastic methanogenesis. *Appl. Environ. Microbiol.* 60:467–72
- Gordon RG, Jurdy DM. 1986. Cenozoic global plate motions. *J. Geophys. Res.* 91:389–406
- Greenwood DR, Basinger JF. 1993. Stratigraphy and floristics of Eocene swamp forests from Axel Heiberg Island, Canadian Arctic Archipelago. *Can. J. Earth Sci.* 30:1914–23
- Greenwood DR, Wing SL. 1995. Eocene continental climates and latitudinal temperature gradients. *Geology* 23:1044–48
- Grimes ST, Hooker JJ, Collinson ME, Matthey DP. 2005. Summer temperatures of late Eocene to early Oligocene freshwaters. *Geology* 33:189–92
- Hall R. 2002. Cenozoic geological and plate tectonic evolution of SE Asia and the SW Pacific: computer-based reconstructions, model and animations. *J. Asian Earth Sci.* 20:353–434
- Helle G, Schleser GH. 2004. Beyond CO₂-fixation by Rubisco—an interpretation of ¹³C/¹²C variations in tree rings from novel intraseasonal studies on broad-leaf trees. *Plant Cell Environ.* 27:367–80
- Higgins JA, Schrag DP. 2006. Beyond methane: towards a theory for the Paleocene-Eocene Thermal Maximum. *Earth Planet. Sci. Lett.* 245:523–37
- Hornibrook ERC, Longstaffe FJ, Fyfe WS. 2000. Factors influencing stable isotope ratios in CH₄ and CO₂ within subenvironments of freshwater. *Isot. Environ. Health Stud.* 36:151–76
- IAEA/WMO. 2006. Global network of isotopes in precipitation. The GNIP Database. <http://isohis.iaea.org>
- Irving E, Wynne PJ. 1991. The Paleolatitude of the Eocene fossil forests of Arctic Canada. In *Tertiary Fossil Forests of the Geodetic Hills, Axel Heiberg Island, Arctic Archipelago*, ed. RL Christie, NJ McMillan, pp. 209–11. Ottawa: Geol. Surv. Can.
- Ivany LC, van Simaey S, Domack EW, Samson SD. 2006. Evidence for an earliest Oligocene ice sheet on the Antarctic Peninsula. *Geology* 34:377–80
- Jagels R, LePage BA, Jiang M. 2001. Definitive identification of *Larix* (Pinaceae) wood based on anatomy from the middle Eocene, Axel Heiberg Island, Canadian High Arctic. *IAWA J.* 22:73–83
- Jagels R, Visscher GE, Lucas J, Goodell B. 2003. Palaeo-adaptive properties of the xylem of *Metasequoia*: mechanical/hydraulic compromises. *Ann. Botany* 92:79–88
- Jahren AH, Byrne M, Sternberg LSL, Summons RE. 2007. No Arctic ice during the Middle Eocene: evidence from the $\delta^{13}\text{C}$ value of *n*-alkanes from Axel Heiberg Island. *Palaeogeogr., Palaeoclimatol., Palaeoecol.* 244:In press
- Jahren AH, LePage BA, Werts SP. 2004. Methanogenesis in Eocene Arctic soils inferred from $\delta^{13}\text{C}$ of tree fossil carbonates. *Palaeogeogr. Palaeoclimatol. Palaeoecol.* 214:347–58
- Jahren AH, Sternberg LSL. 2007. Intraseasonal patterns of carbon storage, precipitation and relative humidity during the Arctic Middle Eocene. *Geology* 35:In press
- Jahren AH, Sternberg LSL. 2002. Eocene meridional weather patterns reflected in the oxygen isotopes of arctic fossil wood. *GSA Today* 1:4–9

- Jahren AH, Sternberg LSL. 2003. Humidity estimate for the middle-Eocene Arctic rainforest. *Geology* 31:463–66
- Kojima S, Sweda T, LePage BA, Basinger JF. 1998. A new method to estimate accumulation rates of lignites in the Eocene Buchanan Lake Formation, Canadian Arctic. *Palaeogeogr. Palaeoclimatol. Palaeoecol.* 141:115–22
- Küsel K, Drake H. 1999. Microbial turnover of low molecular weight organic acids during leaf litter decomposition. *Soil Biol. Biochem.* 31:107–18
- Labandeira CC, LePage BA, Johnson AH. 2001. A *Dendroctonus* bark engraving (Coleoptera: Scolytidae) from a middle Eocene *Larix* (Coniferales: Pinaceae): early or delayed colonization? *Am. J. Botany* 88:2026–39
- Lashof DA, Ahuja DR. 1990. Relative contributions of greenhouse gas emissions to global warming. *Nature* 344:529–31
- LePage BA, Basinger JF. 1991a. A new species of *Larix* (Pinaceae) from the early Tertiary of Axel Heiberg Island, Arctic Canada. *Rev. Palaeobot. Palynol.* 70:89–111
- LePage BA, Basinger JF. 1991b. Early Tertiary *Larix* from the Buchanan Lake Formation, Canadian Arctic Archipelago, and a consideration of the phytogeography of the genus. In *Tertiary Fossil Forests of the Geodetic Hills, Axel Heiberg Island, Arctic Archipelago*, ed. RL Christie, NJ McMillan, pp. 67–81. Ottawa: Geol. Surv. Can.
- LePage BA, Basinger JF. 1995. The evolutionary history of the genus *Larix* (Pinaceae). In *Ecology and Management of Larix Forests: A Look Ahead*, ed. WC Schmidt, KJ McDonald, US Dept. Agr., Forest Serv., Gen. Tech. Rep. GTR-INT-319, pp. 19–29
- Liu YS, Basinger JF. 2000. Fossil *Cathaya* (Pinaceae) pollen from the Canadian High Arctic. *Int. J. Plant Sci.* 161:829–47
- Lowenstein TK, Demicco RV. 2006. Elevated Eocene atmospheric CO₂ and its subsequent decline. *Science* 313:1928
- Ludvigson GA, González LA, Metzger RA, Witzke BJ, Brenner BL, et al. 1998. Meteoric sphaerosiderite lines and their use for paleohydrology and paleoclimatology. *Geology* 26:1039–42
- Luo Y, Sternberg LSL. 1992. Hydrogen and oxygen isotopic fractionation during heterotrophic cellulose synthesis. *J. Exper. Bot.* 43:47–50
- MacLennan J, Jones SM. 2006. Regional uplift, gas hydrate dissociation and the origins of the Paleocene-Eocene Thermal Maximum. *Earth Planet. Sci. Lett.* 245:65–80
- McCarroll D, Loader NJ. 2004. Stable isotopes in tree rings. *Q. Sci. Rev.* 23:771–01
- McIntyre DJ. 1991. Pollen and spore flora of an Eocene forest, eastern Axel Heiberg Island, N.W.T. In *Tertiary Fossil Forests of the Geodetic Hills, Axel Heiberg Island, Arctic Archipelago*, ed. RL Christie, NJ McMillan, pp. 83–97. Ottawa: Geol. Surv. Can.
- McKenna MC. 1980. Eocene paleolatitude, climate, and mammals of Ellesmere Island. *Palaeogeogr. Palaeoclimatol. Palaeoecol.* 30:349–62
- Mora G, Jahren AH. 2003. Isotopic evidence for the role of plant development on transpiration in deciduous forests of southern United States. *Glob. Biogeochem. Cycles* 17:GB1044

- Moran K. 2006. 36 others. The Cenozoic palaeoenvironment of the Arctic Ocean. *Nature* 441:601–5
- Müller RD, Roest WR, Royer JY, Gahagan LM, Sclater JG. 1997. Digital isochrons of the world's ocean floor. *J. Geophys. Res.* 102:3211–14
- Obst JR, McMillan NJ, Blanchette RA, Christensen DJ, Faix O, et al. 1991. Characterization of Canadian Arctic fossil woods. In *Tertiary Fossil Forests of the Geodetic Hills, Axel Heiberg Island, Arctic Archipelago*, ed. RL Christie, NJ McMillan, pp. 123–46. Ottawa: Geol. Surv. Can.
- Pagani M, Zachos JC, Freeman KH, Tipple B, Bohaty S. 2005. Marked decline in atmospheric carbon dioxide concentrations during the Paleogene. *Science* 309:600–3
- Pearson PN, Palmer MR. 2000. Atmospheric carbon dioxide concentrations over the past 60 million years. *Nature* 406:695–99
- Rask HM, Schoenau JJ. 1993. ¹³C natural abundance variations in carbonates and organic carbon from boreal forest wetlands. *Biogeochemistry* 22:23–35
- Retallack G. 2001. A 300-million-year record of atmospheric carbon dioxide from fossil plant cuticles. *Nature* 411:287–90
- Richter S, LePage BA. 2005. A high-resolution palynological analysis, Axel Heiberg Island, Canadian High Arctic. In *The Geobiology and Ecology of Metasequoia*, ed. BA LePage, CJ Williams, H Yang, pp. 137–58. Dordrecht, Neth.: Springer
- Ricketts BD. 1987. Princess Margaret Arch: re-evaluation of an element of the Eurekan Orogen, Axel Heiberg Island, Arctic Archipelago. *Can. J. Earth Sci.* 24:2499–505
- Ricketts BD. 1991. Sedimentation, Eurekan tectonism and the fossil forest succession on eastern Axel Heiberg Island, Canadian Arctic Archipelago. In *Tertiary Fossil Forests of the Geodetic Hills, Axel Heiberg Island, Arctic Archipelago*, ed. RL Christie, NJ McMillan, pp. 1–27. Ottawa: Geol. Surv. Can.
- Roden JS, Ehleringer JR. 1999. Hydrogen and oxygen isotope ratios of tree-ring cellulose for riparian trees grown long-term under hydroponically controlled environments. *Oecologia* 121:467–77
- Roden JS, Lin G, Ehleringer JR. 2000. A mechanistic model for interpretation of hydrogen and oxygen isotope ratios in tree-ring cellulose. *Geochim. Cosmochim. Acta* 64:21–35
- Royer DL. 2006. CO₂-forced climate thresholds during the Phanerozoic. *Geochim. Cosmochim. Acta* 70:5665–75
- Royer DL, Beerling DJ. 2003. Carbon loss by deciduous trees in a CO₂-rich polar environment. *Nature* 424:60–62
- Royer DL, Berner RA, Beerling DJ. 2001. Phanerozoic atmospheric CO₂ change; evaluating geochemical and paleobiological approaches. *Earth Sci. Rev.* 54:349–92
- Royer DL, Wing SL, Beerling DJ, Jolley DW, Koch PL, et al. 2001. Paleobotanical evidence for near present-day levels of atmospheric CO₂ during part of the Tertiary. *Science* 292:2310–13
- Sauer PE, Sternberg LSL. 1994. Improved method for the determination of the oxygen isotopic composition of cellulose. *Anal. Chem.* 66:2409–11

- Schlesinger WH, Bernhardt ES, DeLucia EH, Ellsworth DS, Finzi AC, et al. 2006. The Duke Forest FACE experiment: CO₂ enrichment of a Loblolly Pine forest. In *Managed Ecosystems and CO₂ Case Studies, Processes and Perspectives*, ed. J Nösberger, SP Long, RJ Norby, M Stitt, GR Hendrey, H Blum. Berlin and Heidelberg: Springer-Verlag
- Sessions AL, Jahnke LL, Schimmelmann A, Hayes JM. 2002. Hydrogen isotope fractionation in lipids of the methane-oxidizing bacterium *Methylococcus capsulatus*. *Geochim. Cosmochim. Acta* 66:3955–69
- Sluijs A, Schouten S, Pagani M, Woltering M, Brinkhuis H, et al. 2006. Subtropical Arctic Ocean temperatures during the Palaeocene/Eocene Thermal Maximum. *Nature* 441:610–13
- Sternberg LSL. 1989. Oxygen and hydrogen isotope measurements in plant cellulose analysis. In *Modern Methods of Plant Analysis*, ed. HF Linskens, JF Jackson, pp. 89–99. Heidelberg: Springer-Verlag
- Sternberg LSL, DeNiro MJ, Savidge RA. 1986. Oxygen isotope exchange between metabolites and water during biochemical reactions leading to cellulose synthesis. *Plant Physiol.* 82:423–27
- Sternberg LSL, Pinzon MC, Anderson WT, Jahren AH. 2006. Variation in oxygen isotope fractionation during cellulose synthesis: intramolecular and biosynthetic effects. *Plant Cell Environ.* 29:1881–89
- Sugimoto A, Wada E. 1993. Carbon isotopic composition of bacterial methane in a soil incubation experiment: contributions of acetate and CO₂/H₂. *Geochim. Cosmochim. Acta* 57:4015–27
- Tarnocai C, Kodama H, Fox C. 1991. Characteristics and possible origin of the white layers found in the fossil forest deposits, Axel Heiberg Island. In *Tertiary Fossil Forests of the Geodetic Hills, Axel Heiberg Island, Arctic Archipelago*, ed. RL Christie, NJ McMillan, pp. 189–200. Ottawa: Geol. Surv. Can.
- Tarnocai C, Smith CAS. 1991. Paleosols of the fossil forest area, Axel Heiberg Island. In *Tertiary Fossil Forests of the Geodetic Hills, Axel Heiberg Island, Arctic Archipelago*, ed. RL Christie, NJ McMillan, pp. 171–88. Ottawa: Geol. Surv. Can.
- Ufnar DF, González LA, Ludvigson GA, Brenner BL, Witzke BJ. 2002. The mid-Cretaceous water bearer: isotope mass balance quantification of the Albian hydrologic cycle. *Palaeogeogr. Palaeoclimatol. Palaeoecol.* 188:51–71
- Ufnar DF, Ludvigson GA, González LA, Brenner BL, Witzke BJ. 2004. High latitude meteoric δ¹⁸O compositions: paleosol siderite in the Middle Cretaceous Nanushuk Formation, North Slope, Alaska. *Geol. Soc. Am. Bull.* 116:463–73
- White JWC. 1988. Stable hydrogen isotope ratios in plants: a review of current theory and some potential applications. In *Stable Isotopes in Ecological Research*, ed. PW Rundel, JR Ehleringer, KA Nagy, pp. 142–62. Berlin: Springer-Verlag
- Whiticar MJ, Faber E, Schoell M. 1986. Biogenic methane formation in marine and freshwater environments: CO₂ reduction vs. acetate fermentation—isotopic evidence. *Geochim. Cosmochim. Acta* 50:693–709
- Williams CJ, Johnson AH, LePage BA, Vann DR, Taylor KD. 2003a. Reconstruction of Tertiary *Metasequoia* forests. I. Test of a method for biomass determination based on stem dimensions. *Paleobiology* 29:256–70

- Williams CJ, Johnson AH, LePage BA, Vann DR, Sweda T. 2003b. Reconstruction of Tertiary *Metasequoia* forests. II. Structure, biomass, and productivity of Eocene floodplain forests in the Canadian Arctic. *Paleobiology* 29:271–92
- Wolfe JA. 1994. Alaskan Palaeogene climates as inferred from the CLAMP database. In *Cenozoic Plants and Climates of the Arctic*, ed. MC Boulter, HC Fisher, pp. 223–37. Berlin and New York: Springer-Verlag
- Xu X, Lithgow-Bertelloni CR, Conrad CP. 2006. Global reconstructions of Cenozoic seafloor ages: implications for bathymetry and sea level. *Earth Planet. Sci. Lett.* 243:552–64
- Yakir D, DeNiro MJ. 1990. Oxygen and hydrogen isotope fractionation during cellulose metabolism in *Lemna gibba* L. *Plant Physiol.* 93:325–32
- Yakir D, Sternberg LSL. 2000. The use of stable isotopes to study ecosystem gas exchange. *Oecologia* 123:297–311
- Yang H, Huang Y, Leng Q, LePage BA, Williams CJ. 2005. Biomolecular preservation of Tertiary *Metasequoia* fossil Lagerstätten revealed by comparative pyrolysis analysis. *Rev. Palaeobot. Palynol.* 134:237–56

RELATED RESOURCES

- Beerling DJ, Osborne CP. 2002. Physiological ecology of Mesozoic polar forests in a high CO₂ environment. *Ann. Bot.* 89:329–39
- McIver EE, Basinger JF. 1999. Early Tertiary floral evolution in the Canadian High Arctic. *Ann. Mo. Bot. Gard.* 86:523–45



Contents

Frontispiece	
<i>Robert N. Clayton</i>	xiv
Isotopes: From Earth to the Solar System	
<i>Robert N. Clayton</i>	1
Reaction Dynamics, Molecular Clusters, and Aqueous Geochemistry	
<i>William H. Casey and James R. Rustad</i>	21
The Aral Sea Disaster	
<i>Philip Micklin</i>	47
Permo-Triassic Collision, Subduction-Zone Metamorphism, and Tectonic Exhumation Along the East Asian Continental Margin	
<i>W.G. Ernst, Tatsuki Tsujimori, Ruth Zhang, and J.G. Liou</i>	73
Climate Over the Past Two Millennia	
<i>Michael E. Mann</i>	111
Microprobe Monazite Geochronology: Understanding Geologic Processes by Integrating Composition and Chronology	
<i>Michael L. Williams, Michael J. Jercinovic, and Callum J. Hetherington</i>	137
The Earth, Source of Health and Hazards: An Introduction to Medical Geology	
<i>H. Catherine W. Skinner</i>	177
Using the Paleorecord to Evaluate Climate and Fire Interactions in Australia	
<i>Amanda H. Lynch, Jason Beringer, Peter Kershaw, Andrew Marshall, Scott Mooney, Nigel Tapper, Chris Turney, and Sander Van Der Kaars</i>	215
Wally Was Right: Predictive Ability of the North Atlantic “Conveyor Belt” Hypothesis for Abrupt Climate Change	
<i>Richard B. Alley</i>	241
Microsampling and Isotopic Analysis of Igneous Rocks: Implications for the Study of Magmatic Systems	
<i>J.P. Davidson, D.J. Morgan, B.L.A. Charlier, R. Harlou, and J.M. Hora</i>	273
Balancing the Global Carbon Budget	
<i>R.A. Houghton</i>	313
Long-Term Perspectives on Giant Earthquakes and Tsunamis at Subduction Zones	
<i>Kenji Satake and Brian F. Atwater</i>	349

Biogeochemistry of Glacial Landscape Systems <i>Suzanne Prestrud Anderson</i>	375
The Evolution of Trilobite Body Patterning <i>Nigel C. Hughes</i>	401
The Early Origins of Terrestrial C ₄ Photosynthesis <i>Brett J. Tipple and Mark Pagani</i>	435
Stable Isotope-Based Paleoaltimetry <i>David B. Rowley and Carmala N. Garzione</i>	463
The Arctic Forest of the Middle Eocene <i>A. Hope Jabren</i>	509
Finite Element Analysis and Understanding the Biomechanics and Evolution of Living and Fossil Organisms <i>Emily J. Rayfield</i>	541
Chondrites and the Protoplanetary Disk <i>Edward R.D. Scott</i>	577
Hemispheres Apart: The Crustal Dichotomy on Mars <i>Thomas R. Watters, Patrick J. McGovern, and Rossman P. Irwin III</i>	621
Advanced Noninvasive Geophysical Monitoring Techniques <i>Roel Snieder, Susan Hubbard, Matthew Haney, Gerald Barwden, Paul Hatchell, André Revil, and DOE Geophysical Monitoring Working Group</i>	653
Models of Deltaic and Inner Continental Shelf Landform Evolution <i>Sergio Fagherazzi and Irina Overeem</i>	685
Metal Stable Isotopes in Paleoceanography <i>Ariel D. Anbar and Olivier Rouxel</i>	717
Tectonics and Climate of the Southern Central Andes <i>M.R. Strecker, R.N. Alonso, B. Bookhagen, B. Carrapa, G.E. Hilley, E.R. Sobel, and M.H. Trauth</i>	747

Indexes

Cumulative Index of Contributing Authors, Volumes 25–35	789
Cumulative Index of Chapter Titles, Volumes 25–35	793

Errata

An online log of corrections to *Annual Review of Earth and Planetary Sciences* chapters (if any, 1997 to the present) may be found at <http://earth.annualreviews.org>